JSIAM Letters Vol.10 (2018) pp.65–68 ©2018 Japan Society for Industrial and Applied Mathematics

Shape optimization for a linear elastic fish robot

Wares Chanchareon[1] and Hideyuki Azegami[1]

[1] Nagoya University, A4-2 (780) Furo-cho, Chikusa-ku, Nagoya 464-8601, Japan

E-mail *wares@az.cs.is.nagoya-u.ac.jp*

Received August 29, 2018, Accepted September 11, 2018

Abstract

This paper presents an approach to designing a fish-like linear elastic body whose vibration mode becomes a swimming mode similar to that observed in real fish. To determine the shape of the elastic body, a shape optimization problem is formulated using the squared error norm between the solution of a frequency response and the swimming mode as the cost function and solved by a method based on the H^1 gradient method. The body is excited by body forces located at assigned places. The frequency is set around the natural frequency of the eigenmode, mostly in accordance with the swimming mode.

Keywords shape optimization, fish swimming function, shape derivative, H^1 gradient method

Research Activity Group Mathematical Design

1. Introduction

The locomotion of fish has been mimicked mainly by link mechanisms in artificial fish robots (for an example, see [1]). In this study, a vibration mode of a linear elastic body will be used instead of link mechanisms.

Mathematical analysis of the locomotion of fish was studied by Lighthill [2]. He obtained the result of thrust produced by the fish using the boundary layer theory under the assumption that a slender-bodied fish in inviscid flow produces transverse oscillatory movements wherein amplitude increases from zero over the front portion to a maximum at the tail. Wu [3] discussed the optimum motion with respect to a prescribed thrust at the expense of the minimum work done based on Lighthill's theory.

The swimming modes observed in the locomotion of real fish were reported by Videler and Hess [4–6]. They obtained kinematic data for fast swimming fishes, described the motions with Fourier-series, and computed the kinematic quantities such as the lateral bending moment and power. Based on their study and other literature, Barret [1] used the swimming mode such as

$$\boldsymbol{u}_{\mathrm{R}}(\boldsymbol{x},t)=\boldsymbol{e}_2\left(c_1x_1+c_2x_1^2\right)\sin\left(kx_1+\omega_0 t\right), \quad (1)$$

where $\boldsymbol{u}_{\mathrm{R}}:\Omega_0\times\mathbb{R}\to\mathbb{R}^3$ denotes the transverse displacement at a location $\boldsymbol{x}=(x_i)_i\in\Omega_0\subset\mathbb{R}^3$ with the domain and coordinates shown in Fig. 1, time $t\in\mathbb{R}$, $\boldsymbol{e}_2$ the unit vector in the x_2 direction, $k=2\pi/\lambda$ the wave number, λ the wavelength, ω_0 the undulation frequency, and c_1 and c_2 are constants for the amplitude envelope. Regarding the frequency, Wardle and Videler [7] reported that the muscle activation frequency is similar to the undulation frequency measured using an electromyogram.

Based on the above information, if the shape of a linear elastic body can be determined, whose vibration mode becomes the swimming mode such as (1), we can design a robotic fish whose thrust is produced by the vibration mode of the linear elastic body. In this paper, as the first trial, we formulate the shape optimization problem by neglecting the fluid surrounding the fish and demonstrate the feasibility of this idea with a numerical example.

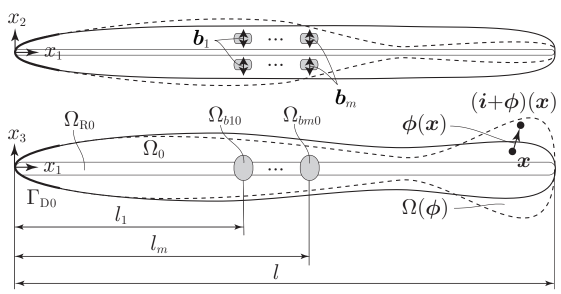

Fig. 1. Swimming fish problem.

2. Domains and design variable

Let us assume that the body of a fish is made of a linear elastic material and defined in $\Omega_0\subset\mathbb{R}^3$ as shown in Fig. 1. We assume that Ω_0 has a Lipschitz boundary $\partial\Omega_0$, $\Gamma_{\mathrm{D0}}\subset\partial\Omega_0$ is a Dirichlet boundary for which the displacement is fixed in accordance with (1) around the origin, and $\Gamma_{\mathrm{N0}}=\partial\Omega_0\setminus\bar{\Gamma}_{\mathrm{D0}}$ ($\bar{(\cdot)}$ denotes a closure) is the traction-free Neumann boundary. In this study, the domain after Ω_0 has moved is formed by a continuous one-to-one onto mapping $\boldsymbol{i}+\boldsymbol{\phi}:\mathbb{R}^d\to\mathbb{R}^d$ as $(\boldsymbol{i}+\boldsymbol{\phi})(\Omega_0)=\{(\boldsymbol{i}+\boldsymbol{\phi})(\boldsymbol{x})|\,\boldsymbol{x}\in\Omega_0\}$ using $\boldsymbol{i}$ as the identity mapping and denoted as $\Omega(\boldsymbol{\phi})$. Similarly, with respect to the initial domain or boundary denoted as $(\,\cdot\,)_0$, $(\,\cdot\,)(\boldsymbol{\phi})$ represents $\{(\boldsymbol{i}+\boldsymbol{\phi})(\boldsymbol{x})|\,\boldsymbol{x}\in(\,\cdot\,)_0\}$. In this study, we set $\boldsymbol{\phi}$ as the design variable for which the Hilbert space and the admissible set are defined as

$$X=\Big\{\boldsymbol{\phi}\in H^1\left(\mathbb{R}^d;\mathbb{R}^d\right)\Big|\ \boldsymbol{\phi}=\boldsymbol{0}_{\mathbb{R}^d}\ \text{on}\ \bar{\Omega}_{\mathrm{R0}}\cup\bar{\Omega}_{b10}\cup\cdots\cup\bar{\Omega}_{bm0}\Big\},$$

$$\mathcal{D} = \left\{ \boldsymbol{\phi} \in X \cap W^{1,\infty}\left(\mathbb{R}^d;\mathbb{R}^d\right) \middle| \boldsymbol{i} + \boldsymbol{\phi} : \text{bijective} \right\},$$

respectively, where $\bar{\Omega}_{\mathrm{R}0} \subset \Omega_0$ is the domain in which the swimming mode $\boldsymbol{u}_{\mathrm{R}}$ in (1) is given. In this study, $\Omega_{\mathrm{R}0}$ is assumed to be the domain along fish's spine. Because the transverse movement in this domain is dominant in the swimming mode. $\bar{\Omega}_{bi0} \subset \Omega_0$ ($i \in \{1,\ldots,m\}$, $\bar{\Omega}_{\mathrm{R}0} \cap \bar{\Omega}_{b10} \cap \cdots \cap \bar{\Omega}_{bm0} = \emptyset$) are domains in which cyclic driving body forces $\boldsymbol{b}_i : \bar{\Omega}_{bi0} \times \mathbb{R} \to \mathbb{R}^d$ are given.

3. State determination problem

We assume a $\boldsymbol{\phi} \in \mathcal{D}$, that is $\Omega(\boldsymbol{\phi})$, is given to formulate a state determination problem of frequency response of the linear elastic body. Let $\boldsymbol{b}_i$ ($i \in \{1,\ldots,m\}$) is given by

$$\boldsymbol{b}_i = \boldsymbol{e}_2\left(c_1 l_i + c_2 l_i^2\right)\sin\left(k l_i + \omega_0 t\right) \quad \text{in } \Omega_{bi0}, \tag{2}$$

where l_i is the length as shown in Fig. 1, and ω_0 and other constants are in accordance with the values in (1). The Fourier transform of $\boldsymbol{b}_i$ is obtained as

$$\mathscr{F}[\boldsymbol{b}_i] = \hat{\boldsymbol{b}}_i^{\mathrm{c}}\delta(\omega+\omega_0) + \hat{\boldsymbol{b}}_i\delta(\omega-\omega_0),$$

where $\delta(\,\cdot\,)$ denotes Dirac's delta function, i is the imaginary unit, $(\,\cdot\,)^{\mathrm{c}}$ the complex conjugate, and

$$\hat{\boldsymbol{b}}_i = \boldsymbol{e}_2\left(c_1 l_i + c_2 l_i^2\right)\mathrm{i}\mathrm{e}^{-\mathrm{i}k l_i}. \tag{3}$$

We use $\boldsymbol{u} : \Omega(\boldsymbol{\phi}) \times \mathbb{R} \to \mathbb{R}^d$ as the displacement when $\boldsymbol{b}_1,\ldots,\boldsymbol{b}_m$ act, and $\hat{\boldsymbol{u}}$ denotes the coefficient function of $\delta(\omega-\omega_0)$ in its Fourier transform. The Hilbert space and the admissible set for $\hat{\boldsymbol{u}}$ are defined as

$$\hat{U} = \left\{ \hat{\boldsymbol{u}} \in H^1\left(\Omega(\boldsymbol{\phi});\mathbb{C}^d\right) \middle| \hat{\boldsymbol{u}} = \boldsymbol{0}_{\mathbb{R}^d} \text{ on } \Gamma_{\mathrm{D}0} \right\},$$

$$\hat{\mathcal{S}} = \hat{U} \cap W^{1,\infty}\left(\Omega(\boldsymbol{\phi});\mathbb{C}^d\right).$$

In this study, we assume $\hat{\boldsymbol{u}}$ is determined in Problem 1 shown later. Here, ρ is the density, which is constant. $\boldsymbol{E}(\hat{\boldsymbol{u}}) = [\boldsymbol{\nabla}\hat{\boldsymbol{u}}^{\mathrm{T}} + (\boldsymbol{\nabla}\hat{\boldsymbol{u}}^{\mathrm{T}})^{\mathrm{T}}]/2$ and $\boldsymbol{S}(\hat{\boldsymbol{u}})$ denote the linear strain and stress, respectively. Let $r = 1 + \mathrm{i}g$ with the structural damping factor g. Moreover, $\chi_{\Omega_{bi0}} : \Omega(\boldsymbol{\phi}) \to \mathbb{R}$ denotes the characteristic function taking the value of 1 in Ω_{bi0} and 0 in $\Omega(\boldsymbol{\phi}) \setminus \bar{\Omega}_{bi0}$. $\boldsymbol{\nu}$ denotes the outer unit normal on $\partial\Omega(\boldsymbol{\phi})$.

Problem 1 (Frequency response by body forces) *Let $\hat{\boldsymbol{b}}_i$ ($i \in \{1,\ldots,m\}$) be given as* (3). *For $\boldsymbol{\phi} \in \mathcal{D}$, find $\hat{\boldsymbol{u}} \in \hat{\mathcal{S}}$ such that*

$$-\omega_0^2\rho\hat{\boldsymbol{u}}^{\mathrm{T}} - r\nabla^{\mathrm{T}}\boldsymbol{S}(\hat{\boldsymbol{u}}) = \sum_{i=1}^{m}\chi_{\Omega_{bi0}}\hat{\boldsymbol{b}}_i \quad \text{in } \Omega(\boldsymbol{\phi}),$$

$$r\boldsymbol{S}(\hat{\boldsymbol{u}})\boldsymbol{\nu} = \boldsymbol{0}_{\mathbb{R}^d} \quad \text{on } \Gamma_{\mathrm{N}}(\boldsymbol{\phi}).$$

4. Shape optimization problem

Using the design variable $\boldsymbol{\phi} \in \mathcal{D}$ and the solution $\hat{\boldsymbol{u}} \in \hat{\mathcal{S}}$ of Problem 1, a shape optimization problem can be constructed. In accordance with the objective of this paper, we use an objective cost function for minimization as

$$f(\boldsymbol{\phi},\alpha,\hat{\boldsymbol{u}}) = \pi\int_{\Omega_{\mathrm{R}0}}\int_{-\infty}^{\infty}\|\boldsymbol{u} - \alpha\boldsymbol{u}_{\mathrm{R}}\|_{\mathbb{R}^3}^2\,\mathrm{d}t\mathrm{d}x$$

$$= \int_{\Omega_{\mathrm{R}0}}(\hat{\boldsymbol{u}} - \alpha\hat{\boldsymbol{u}}_{\mathrm{R}})\cdot(\hat{\boldsymbol{u}} - \alpha\hat{\boldsymbol{u}}_{\mathrm{R}})^{\mathrm{c}}\,\mathrm{d}x, \tag{4}$$

where $\hat{\boldsymbol{u}}_{\mathrm{R}}$ is given as

$$\hat{\boldsymbol{u}}_{\mathrm{R}} = \boldsymbol{e}_2\left(c_1 x_1 + c_2 x_1^2\right)\mathrm{i}\mathrm{e}^{-\mathrm{i}k x_1} \quad \text{in } \Omega_{\mathrm{R}0},$$

and $\alpha \in \mathbb{R}$ is a variable to adjust the magnitude of $\hat{\boldsymbol{u}}_{\mathrm{R}}$ to fit $\hat{\boldsymbol{u}}$. In (4), the second identity is obtained using Parseval's formula.

Using the cost function, we formulate the shape optimization problem as follows.

Problem 2 (Swimming error minimization) *With respect to f in* (4), *find $\boldsymbol{\phi}$ that satisfies*

$$\min_{(\boldsymbol{\phi},\hat{\boldsymbol{u}})\in\mathcal{D}\times\hat{\mathcal{S}}}\left\{ f(\boldsymbol{\phi},\alpha,\hat{\boldsymbol{u}}) \middle| \textit{Problem 1} \right\}. \tag{5}$$

5. Shape derivative of cost function

To solve Problem 2, an iterative scheme using a gradient method will be applied. The gradient of f with respect to an arbitrary domain variation can be evaluated using the Lagrange multiplier method using

$$\mathscr{L}(\boldsymbol{\phi},\alpha,\hat{\boldsymbol{u}},\hat{\boldsymbol{v}}^{\mathrm{c}}) = f(\boldsymbol{\phi},\alpha,\hat{\boldsymbol{u}}) + 2\mathrm{Re}\left[\mathscr{L}_{\mathrm{S}}(\boldsymbol{\phi},\hat{\boldsymbol{u}},\hat{\boldsymbol{v}}^{\mathrm{c}})\right], \tag{6}$$

as the Lagrange function for f. Here $\hat{\boldsymbol{v}}^{\mathrm{c}} \in \mathcal{S}$ is the Lagrange multiplier with respect to Problem 1, and $\mathscr{L}_{\mathrm{S}}(\boldsymbol{\phi},\hat{\boldsymbol{u}},\hat{\boldsymbol{v}}^{\mathrm{c}})$ is the Lagrange function of Problem 1 defined as

$$\mathscr{L}_{\mathrm{S}}(\boldsymbol{\phi},\hat{\boldsymbol{u}},\hat{\boldsymbol{v}}^{\mathrm{c}}) = \int_{\Omega(\boldsymbol{\phi})}\Big(\omega_0^2\rho\hat{\boldsymbol{u}}\cdot\hat{\boldsymbol{v}}^{\mathrm{c}} - r\boldsymbol{S}(\hat{\boldsymbol{u}})\cdot\boldsymbol{E}(\hat{\boldsymbol{v}}^{\mathrm{c}}) + \sum_{i=1}^{m}\chi_{\Omega_{bi0}}\hat{\boldsymbol{b}}_i\cdot\hat{\boldsymbol{v}}^{\mathrm{c}}\Big)\mathrm{d}x. \tag{7}$$

The Fréchet derivative of $\mathscr{L}_{\mathrm{S}}$ with respect to arbitrary variation $(\boldsymbol{\varphi},\tilde{\alpha},\tilde{\hat{\boldsymbol{u}}},\tilde{\hat{\boldsymbol{v}}}^{\mathrm{c}}) \in X \times \mathbb{R} \times \hat{U}^2$ of $(\boldsymbol{\phi},\alpha,\hat{\boldsymbol{u}},\hat{\boldsymbol{v}}^{\mathrm{c}})$ can be obtained as

$$\begin{aligned}\mathscr{L}'(\boldsymbol{\phi},\alpha,\hat{\boldsymbol{u}},\hat{\boldsymbol{v}}^{\mathrm{c}})\left[\boldsymbol{\varphi},\tilde{\alpha},\tilde{\hat{\boldsymbol{u}}},\tilde{\hat{\boldsymbol{v}}}^{\mathrm{c}}\right] &= \mathscr{L}_{\boldsymbol{\phi}}(\boldsymbol{\phi},\alpha,\hat{\boldsymbol{u}},\hat{\boldsymbol{v}}^{\mathrm{c}})[\boldsymbol{\varphi}] + \mathscr{L}_{\alpha}(\boldsymbol{\phi},\alpha,\hat{\boldsymbol{u}},\hat{\boldsymbol{v}}^{\mathrm{c}})[\tilde{\alpha}] \\ &\quad + \mathscr{L}_{\hat{\boldsymbol{u}}}(\boldsymbol{\phi},\alpha,\hat{\boldsymbol{u}},\hat{\boldsymbol{v}}^{\mathrm{c}})\left[\tilde{\hat{\boldsymbol{u}}}\right] + \mathscr{L}_{\hat{\boldsymbol{v}}^{\mathrm{c}}}(\boldsymbol{\phi},\alpha,\hat{\boldsymbol{u}},\hat{\boldsymbol{v}}^{\mathrm{c}})\left[\tilde{\hat{\boldsymbol{v}}}^{\mathrm{c}}\right].\end{aligned} \tag{8}$$

The 4th term of the right-hand side of (8) becomes

$$\mathscr{L}_{\hat{\boldsymbol{v}}_0^{\mathrm{c}}}(\boldsymbol{\phi},\alpha,\hat{\boldsymbol{u}},\hat{\boldsymbol{v}}^{\mathrm{c}})\left[\tilde{\hat{\boldsymbol{v}}}^{\mathrm{c}}\right] = \mathscr{L}_{\mathrm{S}}\left(\boldsymbol{\phi},\alpha,\hat{\boldsymbol{u}},\tilde{\hat{\boldsymbol{v}}}^{\mathrm{c}}\right). \tag{9}$$

Then, if $\boldsymbol{u}$ is a weak solution of Problem 1, this term becomes 0. The 3rd term of the right-hand side of (8) is

$$\begin{aligned}\mathscr{L}_{\hat{\boldsymbol{u}}}(\boldsymbol{\phi},\alpha,\hat{\boldsymbol{u}},\hat{\boldsymbol{v}}^{\mathrm{c}})\left[\tilde{\hat{\boldsymbol{u}}}\right] &= \int_{\Omega(\boldsymbol{\phi})}2\mathrm{Re}\left[\omega_0^2\rho\hat{\boldsymbol{v}}^{\mathrm{c}}\cdot\tilde{\hat{\boldsymbol{u}}} - r\boldsymbol{S}(\hat{\boldsymbol{v}}^{\mathrm{c}})\cdot\boldsymbol{E}\left(\tilde{\hat{\boldsymbol{u}}}\right)\right] \\ &\quad + 2\chi_{\Omega_{\mathrm{R}0}}(\hat{\boldsymbol{u}} - \alpha\hat{\boldsymbol{u}}_{\mathrm{R}})^{\mathrm{c}}\cdot\tilde{\hat{\boldsymbol{u}}}\,\mathrm{d}x.\end{aligned} \tag{10}$$

If $\hat{\boldsymbol{v}}^{\mathrm{c}}$ is a weak solution of the following problem, the 3rd term becomes 0.

Problem 3 (Adjoint problem for f) *Let $\hat{\boldsymbol{u}}$ be the solution of Problem 1. Find $\hat{\boldsymbol{v}}^{\mathrm{c}} \in \mathcal{S}$ such that*

$$-\omega_0^2\rho\hat{\boldsymbol{v}}^{\mathrm{cT}} - r\nabla^{\mathrm{T}}\boldsymbol{S}(\hat{\boldsymbol{v}}^{\mathrm{c}}) = 2\chi_{\Omega_{\mathrm{R}0}}(\hat{\boldsymbol{u}} - \alpha\hat{\boldsymbol{u}}_{\mathrm{R}})^{\mathrm{T}} \quad \text{in } \Omega(\boldsymbol{\phi}),$$

$$r\boldsymbol{S}(\hat{\boldsymbol{v}}^{\mathrm{c}})\boldsymbol{\nu} = \boldsymbol{0}_{\mathbb{R}^d} \quad \text{on } \Gamma_{\mathrm{N}}(\boldsymbol{\phi}).$$

The 2nd term of the right-hand side of (8) is

$$\begin{aligned}&\mathscr{L}_{\alpha}\left(\boldsymbol{\phi},\alpha,\hat{\boldsymbol{u}},\hat{\boldsymbol{v}}^{\mathrm{c}}\right)[\tilde{\alpha}]\\&=\int_{\Omega_{\mathrm{R0}}}2\left(\alpha\hat{\boldsymbol{u}}_{\mathrm{R}}\cdot\hat{\boldsymbol{u}}_{\mathrm{R}}^{\mathrm{c}}-\mathrm{Re}\left[\hat{\boldsymbol{u}}\cdot\hat{\boldsymbol{u}}_{\mathrm{R}}^{\mathrm{c}}\right]\right)\mathrm{d}x. \qquad (11)\end{aligned}$$

Then, if the following holds, the 2nd term becomes 0.

$$\alpha=\frac{\int_{\Omega_{\mathrm{R0}}}\mathrm{Re}\left[\hat{\boldsymbol{u}}\cdot\hat{\boldsymbol{u}}_{\mathrm{R}}^{\mathrm{c}}\right]\mathrm{d}x}{\int_{\Omega_{\mathrm{R0}}}\hat{\boldsymbol{u}}_{\mathrm{R}}\cdot\hat{\boldsymbol{u}}_{\mathrm{R}}^{\mathrm{c}}\mathrm{d}x} \qquad (12)$$

When $(\hat{\boldsymbol{u}},\hat{\boldsymbol{v}}^{\mathrm{c}})\in\mathcal{S}^2$ are the solutions of Problems 1 and 3, the first term on the right-hand side of (8) coincides with the shape derivative of f satisfying the equality constraint of Problem 1. Hence, using the formulae [8, Propositions 9.3.4 and 9.3.7] and $\boldsymbol{\phi}=\mathbf{0}_{\mathbb{R}^d}$ on $\bar{\Omega}_{\mathrm{R0}}\cup\bar{\Omega}_{b10}\cup\cdots\cup\bar{\Omega}_{bm0}$ in $\mathcal{D}$, we have

$$\begin{aligned}\mathscr{L}_{\boldsymbol{\phi}}\left(\boldsymbol{\phi},\alpha,\hat{\boldsymbol{u}},\hat{\boldsymbol{v}}^{\mathrm{c}}\right)[\boldsymbol{\varphi}]&=\langle\boldsymbol{g},\boldsymbol{\varphi}\rangle\\&=\int_{\Omega(\boldsymbol{\phi})}\left(\boldsymbol{G}_{\Omega}\cdot\boldsymbol{\nabla}\boldsymbol{\varphi}^{\mathrm{T}}+g_{\Omega}\boldsymbol{\nabla}\cdot\boldsymbol{\varphi}\right)\mathrm{d}x, \qquad (13)\end{aligned}$$

where

$$\boldsymbol{G}_{\Omega}=2\mathrm{Re}\left[r\left[\boldsymbol{S}\left(\hat{\boldsymbol{u}}\right)\left(\boldsymbol{\nabla}\hat{\boldsymbol{v}}^{\mathrm{cT}}\right)^{\mathrm{T}}+\boldsymbol{S}\left(\hat{\boldsymbol{v}}^{\mathrm{c}}\right)\left(\boldsymbol{\nabla}\hat{\boldsymbol{u}}^{\mathrm{T}}\right)^{\mathrm{T}}\right]\right],$$

$$g_{\Omega}=2\mathrm{Re}\left[\omega_0^2\rho\boldsymbol{u}\cdot\boldsymbol{v}_0^{\mathrm{c}}-r\boldsymbol{S}\left(\boldsymbol{u}\right)\cdot\boldsymbol{E}\left(\boldsymbol{v}_0^{\mathrm{c}}\right)\right].$$

6. Solution

Using the shape gradient $\boldsymbol{g}$ in (13), we use an iterative scheme based on the H^1 gradient method [8, Section 9.9.1]. For $k\in\{0,1,2,\dots\}$, we calculate $\boldsymbol{\phi}_{k+1}=\boldsymbol{\phi}_k+\boldsymbol{\varphi}_g$ using the solution $\boldsymbol{\varphi}_g\in X$ that satisfies

$$c_a a_X\left(\boldsymbol{\varphi}_g,\boldsymbol{\psi}\right)=-\langle\boldsymbol{g},\boldsymbol{\psi}\rangle\quad\forall\boldsymbol{\psi}\in X. \qquad (14)$$

Here c_a is a positive constant to control $\left\|\boldsymbol{\varphi}_g\right\|$ and

$$a_X\left(\boldsymbol{\varphi}_g,\boldsymbol{\psi}\right)=\int_{\Omega(\boldsymbol{\phi})}\boldsymbol{S}\left(\boldsymbol{\varphi}_g\right)\cdot\boldsymbol{E}\left(\boldsymbol{\psi}\right)\mathrm{d}x, \qquad (15)$$

where $\boldsymbol{E}(\,\cdot\,)$ and $\boldsymbol{S}(\,\cdot\,)$ are the linear strain and stress tensors used in Problems 1 and 3, respectively.

7. Numerical example

We developed a computer program that follows the scheme shown in Section 6 using our in-house library. The finite element method was employed to solve Problems 1, 3, and the H^1 gradient method of (14). Fig. 2 shows the initial finite element model with 8,200 quadratic tetrahedral elements and 13,000 nodes. In this study, we set $m=2$, $(l,l_1,l_2)=(0.3,0.12,0.29)$ m and the domains of Ω_{R0}, Ω_{b10} and Ω_{b20} as shown in Fig. 3. The driving frequency $\omega_0/(2\pi)$ was decided to be 2.3 Hz at which the magnitude of $\hat{u}_2$ at the center of Ω_{b10} was maximized under the condition of vibration mode being close to the swimming mode. $c_1=0.002$, $c_2=0.008$ and $\lambda=1.048$ were used by referring to [9, Chapter 3]. In Problems 1 and 3, we used 0.04 MPa and 0.3 for Young's modulus and Poisson's ratio, respectively, $\rho=1{,}080$ kg/m^3 according to Barret's study [1] and $g=0.2$. In (14), c_a was chosen to satisfy Armijo's criterion [8, Definition 3.4.4].

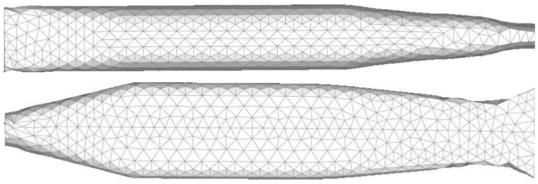

Fig. 2. Initial finite element model: top and side views.

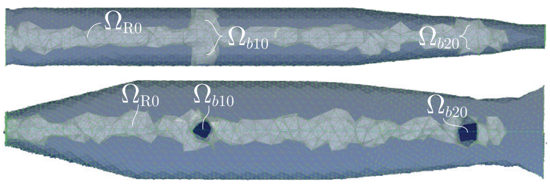

Fig. 3. Domains of Ω_{R0}, Ω_{b10}, Ω_{b20} and Ω_{b30}: top and side views.

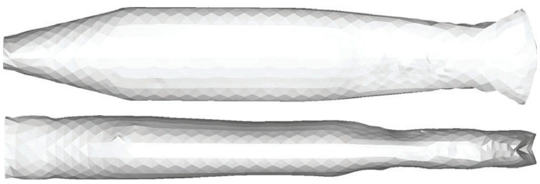

Fig. 4. Optimized shape: top and side views.

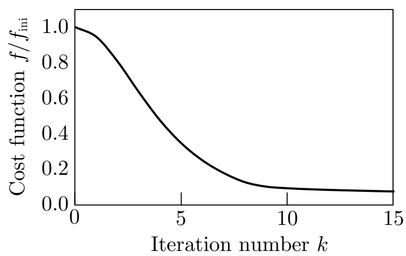

Fig. 5. Iteration history of objective cost function f.

Fig. 4 shows the optimized shape. The iteration history of f decreasing monotonically is shown in Fig. 5. The variation in horizontal displacement of $\boldsymbol{u}_{\mathrm{R}}$ on $(x_1,0,0)$, which denotes $u_2(x_1,t)$, at $\omega_0 t=1$ with respect to shape variation are illustrated in Fig. 6 together with $u_{\mathrm{R}2}(x_1,t)$ in (1). $u_2(x_1,t)$ are defined as follows. Let $\hat{u}_2(x_1)$ denote the second element of $\hat{\boldsymbol{u}}$ on $(x_1,0,0)$, and be converted with amplitude $\bar{u}_2(x_1)$ and phase $\theta(x_1)$ as

$$\hat{u}_2(x_1)=\bar{u}_2(x_1)\,\mathrm{i}\mathrm{e}^{-\mathrm{i}\theta(x_1)},\quad\theta(x_1)=\tan^{-1}\frac{\mathrm{Re}\left[\hat{u}_2(x_1)\right]}{\mathrm{Im}\left[\hat{u}_2(x_1)\right]}.$$

From $\hat{u}_2(x_1)$, we define

$$\begin{aligned}u_2(x_1,t)&=\mathscr{F}^{-1}\left[\hat{u}_2^{\mathrm{c}}(x_1)\,\delta(\omega+\omega_0)+\hat{u}_2(x_1)\,\delta(\omega-\omega_0)\right]\\&=\frac{1}{2\pi}\bar{u}_2(x_1)\sin\left(\theta(x_1)+\omega_0 t\right).\end{aligned}$$

From the comparison of the modes in Fig. 6, we observed that the vibration mode of the initial model did not approach the swimming mode, whereas the vibration mode at the optimized model approached the swimming mode.

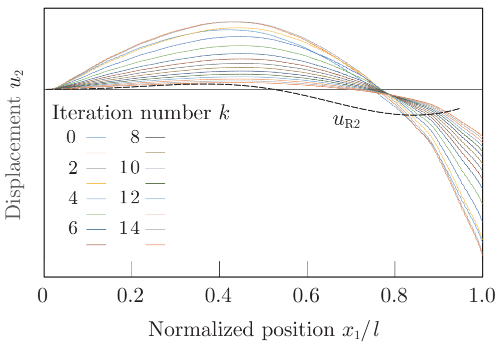

Fig. 6. Iteration history of $u_2(x_1, t)$ at $\omega_0 t = 0$.

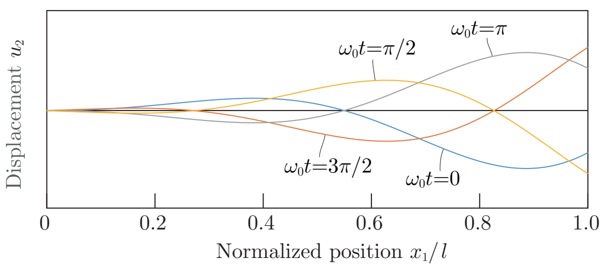

(a) $u_{R2}(x_1, t)$ of (1)

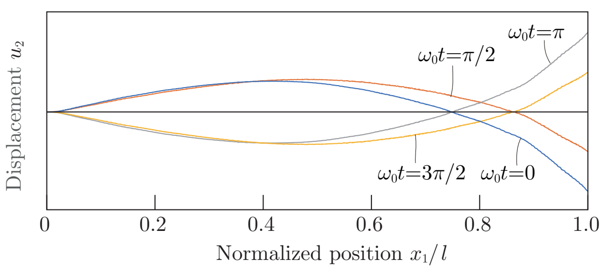

(b) $u_2(x_1, t)$ of initial model

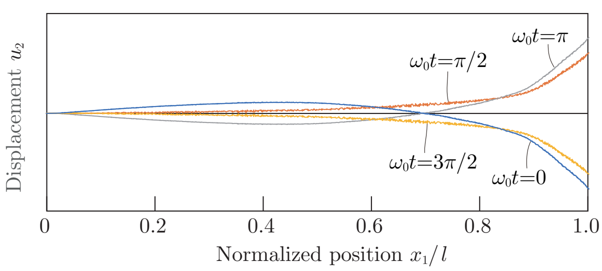

(c) $u_2(x_1, t)$ of optimized model

Fig. 7. Vibration modes with respect to time.

8. Discussion

From the results of Figs. 5 and 6, it can be confirmed that the presented approach finds a mode closer to the vibration mode than to the swimming mode. However, from the time variation of vibration modes shown in Fig. 7, the optimized model (c) is not near $u_{R2}(x_1, t)$ in (a), whereas it is near that of the initial model in (b). A likely candidate of the difference can be considered given that the surrounding fluid is ignored. In a future study, we will investigate the effect of fluids around a fish's body.

Acknowledgments

This work was supported by JSPS KAKENHI (Grant Numbers JP16K05285 and JP17K05140).

References

[1] D. S. Barret, M. S. Triantafyllou, D. K. P. Yue, M. A. Grosenbaugh and M. J. Wolfgang, Drag reduction in fish-like locomotion, J. Fluid Mech., **392** (1999), 183–212.
[2] M. J. Lighthill, Note on the swimming of slender fish, J. Fluid Mech., **9** (1960), 306–317.
[3] T. Y. T. Wu, Hydromechanics of swimming propulsion, part 3, swimming and optimum movements of slender fish with side fins, J. Fluid Mech., **46** (1971), 545–568.
[4] J. J. Videler and F. Hess, Fast continuous swimming of two pelagic predators, saithe (pollachius virens) and mackerel (scomber scombrus): a kinematic analysis, J. exp. Biol., **109** (1984), 209–228.
[5] F. Hess and J. J. Videler, Fast continuous swimming of saithe (pollachius virens): a dynamic analysis of bending moments and muscle power, J. exp. Biol., **109** (1984), 229–251.
[6] J. J. Videler, Fish Swimming, Chapman and Hall, London, 1993.
[7] C. S. Wardle and J. J. Videler, The timing of the EMG in the lateral myotomes of mackerel and saithe at different swimming speeds, J. Fish Biol., **109** (1993), 229–251.
[8] H. Azegami, Shape optimization problems (in Japanese), Morikita Publishing Co., Ltd., Tokyo, 2016.
[9] D. Barrett, Propulsive efficiency of a flexible hull underwater vehicle, PhD thesis, Department of Ocean Engineering, Massachusetts Institute of Technology, Boston, USA, 1996.